The Journal of Experimental Biology 213, 3778-3786

doi:10.1242/jeb.046417

Regulation of conduction velocity in axons from near-field receptors of the crayfish antennule

DeForest Mellon, Jr

Department of Biology, Gilmer Hall, University of Virginia, Charlottesville, VA 22903, USA

dm6d@virginia.edu

Accepted 23 August 2010

SUMMARY

The antennular flagella of the crayfish *Procambarus clarkii* each possess a linear array of near-field receptors, termed standing feathered sensilla, that are extremely sensitive to movement of the surrounding water. Previously it had been shown that, within each flagellum, the axonal conduction velocity of the sensory neuron pair associated with each feathered sensillum was linearly related to the position of the sensillum along the flagellar axis. In the current studies I show that the conduction velocity of axons within the proximal three segments of the antennules, between the flagellum and the brain, is somewhat higher than the corresponding conduction velocity of the same axons in the flagellum, especially for those whose flagellar conduction velocity is between 1 and 3 m s^{-1}, even though there is no net change in axonal diameter within this part of the afferent pathway. One consequence of this change in axonal conduction properties is an effective compression of the temporal spread – potentially by as much as tenfold – which otherwise would occur in arrival times of initial spikes from each sensillum following a mechanical stimulus to the antennule. Furthermore, the pattern signature of initial spike volleys at the brain following a global hydrodynamic stimulus to the flagellum is remarkably consistent and conceivably could be recognized as such by central processing centers. I conclude that conduction velocity adjustments improve temporal summation and resolution from input volleys that originate in the highly sensitive and, hence, inherently noisy near-field receptors, thereby more effectively triggering startle response circuitry at the approach of potential predators.

Key words: antennule, sensilla, axon, latency.

INTRODUCTION

The biramous antennules (first antennae) of freshwater crayfish possess batteries of cuticular sense organs arrayed linearly along the paired lateral and medial flagella. These include olfactory (aesthetasc) sensilla on the distal half of the lateral flagellum, and both near-field hydrodynamic sensilla and presumed dual-function contact mechano-chemosensitive sensilla on both the lateral and medial flagella (Sandeman and Luff, 1974; Tierney et al., 1986; Mellon, 1997) (DeF.M. and V. E. Alones, unpublished observations). With the exception of the near-field sensilla noted below, none of these structures has been directly examined physiologically in crayfishes. Mellon and Christison-Lagay (Mellon and Christison-Lagay, 2008) recently carried out electrophysiological studies of near-field receptors designated as standing feathered sensilla on the antennules of the crayfish *Procambarus clarkii*. Standing feathered sensilla are highly sensitive, sparsely distributed structures that respond to near-field hydrodynamic stimulation. They are of particular interest because their axons exhibit mean conduction velocities (CVs) that are linearly – or nearly linearly – proportional to the sensillum distance from the flagellum base. We hypothesized that conduction velocity regulation might result from different rates of increase in axonal diameter as a function of sensillar position along the flagella; by this reasoning, the oldest, distal sensillar axons, having grown for the longest time periods, would have increased their diameters between the sensilla and the base to larger final values than proximal sensillar axons. In theory, we reasoned, this could assure that action potentials evoked by hydrodynamic wave fronts impinging upon the antennular flagella would arrive at the brain simultaneously and would be maximally effective in evoking startle reflex behaviors. Although anatomical determination of direct synaptic connections between axons of standing feathered sensilla and brain neurons has not been accomplished, behavioral observations of startle responses evoked in freely moving, antenna-deprived *P. clarkii* by an object dropped onto the water surface near the animals' antennules suggested that they are highly sensitive; the animals responded with a backwardly directed tail flip to abrupt hydrodynamic stimulation, or to pairs of electrical stimuli delivered to the respective antennules within a time frame of 50 ms (Mellon and Christison-Lagay, 2008).

The present investigation was undertaken to further examine CV regulation in the antennular axonal pathways serving near-field hydrodynamic sensing, and to determine whether action potentials generated simultaneously at feathered sensilla all along the flagellar arrays would arrive at the brain coincidently. Simple calculations of possible outcomes of mean conduction velocity measurements at the flagellum base, however, instead suggested the possibility of a large disparity in initial spike arrival times at the brain, from as little as 4 ms after passing the flagellum base in the case of the axons originating most distally, to more than 40 ms in the case of axons originating near the base. The results reported here indicate that this degree of temporal dispersion at the brain does not occur, apparently because of changes in axonal CV in the proximal segment of the afferent pathway, between the base of the flagella and the brain, and affecting primarily axons having CV values in the mid range. The consequence of this regulation is that initial afferent spikes originating from approximately 95% of the feathered sensilla arrive at the brain within 5 ms of each other, generating predictable and

highly reproducible patterns of spike volleys. This should not only enable spatial summation of activity from simultaneously stimulated feathered sensilla all along the antennular flagellum, but it may also provide a recognizable temporal initial spike signature to the brain following a global stimulus, increasing the probability of a startle response being generated following potentially threatening hydrodynamic stimuli.

MATERIALS AND METHODS

Animals used were large (45–55 mm carapace length) adult individuals of the freshwater crayfish *Procambarus clarkii* Girard obtained from a supplier in southern Louisiana (Atchafalaya Biological Supply, Raceland, LA 70394, USA). Animals were kept in a culture system (Marine Biotech, Inc., Beverly, MA, USA) featuring filtered, circulating freshwater at 19–20°C and in a 12 h:12 h light:dark photoperiod. They were fed three times per week on frog chow.

Latency measurements were obtained using extracellular suction electrodes that recorded spiking activity simultaneously at the entrance of the antennular nerve to the brain and from the branch of the antennular nerve at the base of the medial flagellum, in highly dissected isolated head preparations. Preparations were fastened to the Sylgard floor of a circular pool of crayfish saline (composition, in mmol l^{-1}: NaCl, 205; KCl, 5.4; $CaCl_2.2H_2O$ 13.6; $MgCl_2.7H_2O$ 2.7; $NaHCO_3$ 2.4; pH adjusted to 7.4 with HCl) through which flowed chilled crayfish saline at a temperature of 16±0.3°C. Activity from the antennular nerve was recorded *via* capillary suction electrodes placed as discussed above, following dissection of the ventral aspects of the first (coxopodite) and third (ischiopodite) segments of the antennule. For technical reasons it was easier to record from the medial branch or fasciculation of the antennular nerve, and so all data were obtained exclusively from sensilla on the medial flagellum. The electrodes were fitted to suction-capable holders and connected to the inputs of a Grass P-511 and a Grass P-15 low-level AC preamplifier (Astro Med, Inc., West Warwick, RI, USA). Input signals were frequency-filtered between 1 Hz and 3 kHz and acquired using Pclamp 8.2 computer software (Axon Instruments, Inc, Foster City, CA, USA). Mean latency values for spikes associated with each identified sensillum were obtained from twenty mechanical stimuli delivered at 1 Hz. The extracellularly recorded spike waveforms, corresponding to activity at the two sites, were identified by response consistency following repeated stimulation of a visually identified standing feathered sensillum. Mechanical stimuli were applied with a small insect pin probe driven by a small-diameter audio speaker controlled by a Grass stimulator. The probe was manipulated to contact the sensillum, which was always signaled by a dramatic increase in spiking activity due to minute vibrations originating in the speaker cone. Then the probe was backed off until contact was lost, remaining at a distance of about 10 µm from the sensillum. Stimuli were 2-ms duration rectangular pulses driven using a voltage setting of 5 through a stimulus isolation unit. This setting produced an axial movement of the stimulus probe by a maximum of 20 µm as viewed through a compound microscope, using a duration of 20 ms; at a duration of 2 ms the probe displacement occurred too rapidly to be visualized, but it certainly could not have been more than 20 µm. No attempt was made to determine the rate of change of position of the probe, since the same settings were used to compare sensillum-to-base CVs and sensillum-to-brain CVs. CV values were calculated from the initial spike latency and the distance of the sensillum from the recording electrode just adjacent to the proximal margin of the basal annulus of the flagellum, as well as from the recording point at the entrance of the nerve to the brain.

For comparisons of mechanically and electrically evoked response latencies, intracellular recordings of spiking activity in feathered sensillar afferents were also obtained from axons within the antennular nerve, either near the brain or at the base of the flagella, using glass micropipettes filled with 1 mol l^{-1} KCl, with an electrical resistances of 10–25 MΩ. Recordings measured the difference between the spike latency, following standard speaker stimuli, and the latency in the same axon evoked by a just-suprathreshold 0.1-ms electrical shock delivered to the flagellum after surgically truncating it beyond the annulus distal to the sensillum under examination (see Table 1). The differences in latency from individual sensilla measured by these two methods varied between 0.31 and 2.21 ms among the eleven axons, with the latency following electrical stimulation always being smaller than that occurring after mechanical stimulation. There was no obvious correlation between latency difference and sensillar position along the flagellum, or between the temperatures of the saline bath during an experiment.

Anatomical observations were made on antennular flagella or antennular nerve segments transected into 2–3 mm identified lengths (sub-segments) that were subsequently fixed in 4% glutaraldehyde made up in 0.1 mol l^{-1} sodium cacodylate buffer. Fixation took place at 4°C overnight, after which the tissue fragments were washed in fresh chilled buffer and post-fixed in 1% osmium tetroxide, dehydrated and embedded in plastic. Thick (0.5 µm) sections were cut with glass knives from the proximal end of each sub-segment and subsequently stained with Toluidine Blue. Images of appropriate sections were taken using a Zeiss Axiophot compound microscope and cross-sectional areas of selected axons were obtained with ImageJ software. Equivalent diameters of circular areas were calculated by dividing by π.

RESULTS

Antennular anatomy

The composite illustration in Fig. 1 shows some of the anatomical features of the crayfish antennule. Fig. 1A is a lateral view of a right-hand antennule from a young crayfish. The lateral (LF) and medial (MF) flagella are indicated in approximately normal postures for a resting animal. A scanning electron micrograph of a standing feathered sensillum (thick white arrow) on a flagellum is shown in Fig. 1B. Each feathered sensillum is supplied with two sensory neurons that have, respectively, preferred sensitivity in either the distal or the proximal direction of movement, but which also respond with slightly less sensitivity to lateral movements (Mellon and Christison-Lagay, 2008). Asterisks indicate structures I have termed beaked sensilla, presumed contact mechano-chemoreceptor sensilla (DeF.M., unpublished data). Fig. 1C is a drawing of the basal three segments (I–III) from a right-hand antennule of an adult animal. The lateral and medial flagella are truncated in the drawing, but were, respectively, 30 and 27 mm long. The three basal segments together were 14 mm long, thus constituting approximately 32% of the entire antennular length. Observations in other animals confirmed that the three basal segments constitute 30–40% of the length of the antennule.

Recording techniques

As in our previous electrophysiological studies of the crayfish antennule (Mellon, 1997; Mellon and Christison-Lagay, 2008), the techniques I used never recorded electrical activity in the antennular nerve following chemical or mechanical stimulation of either the aesthetasc sensilla or the beaked sensilla; the very low-amplitude signals from these tiny (0.2–5 µm diameter) axons were lost in the amplifier noise level. However, large (0.5–2 mV) amplitude

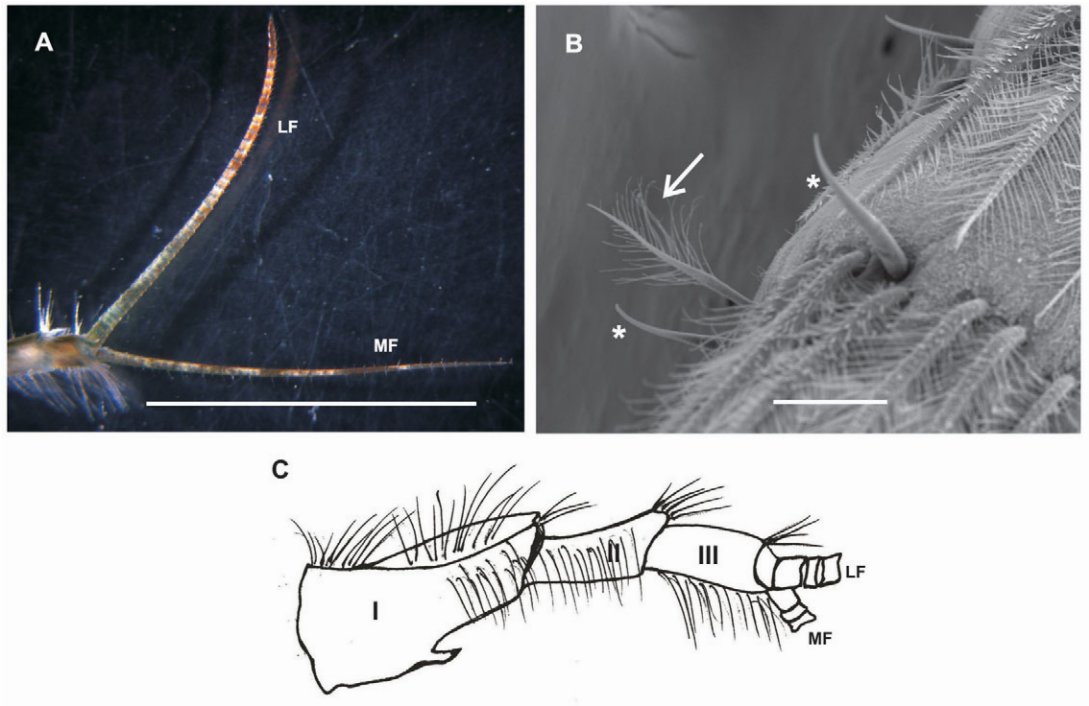

Fig. 1. (A) A right-hand *Procambarus* antennule with a lateral flagellum (LF) and medial flagellum (MF), approximately 1.5 cm long. (B) A scanning electron micrograph showing a standing feathered sensillum (arrow), and three beaked sensilla (*). (C) A diagram of the three basal antennular segments (I–III). See text for details. Scale bars, 500 μm (A); 100 μm (B).

spontaneous spiking activity was invariably recorded following placement of the suction electrodes in response to small disturbances within the saline bath, as well as to mechanical stimulation of individual standing feathered sensilla, indicating that these structures must be supplied by the largest axons in the antennular nerve. Fig. 2A illustrates simultaneous electrical recordings, in the absence of obvious stimulation, obtained with suction electrodes from the branch of the antennular nerve just proximal to the basal annulus of the medial flagellum (upper trace) and from where the nerve enters the brain (lower trace). High levels of spontaneous activity from feathered sensillar axons are a common observation in this preparation, undoubtedly because of the high sensitivity of the near-field receptors. Fig. 2B shows records from the medial nerve branch at the brain entrance in another preparation, illustrating superimposed responses (cyan traces) to ten consecutive 100-ms mechanical pulses delivered by a circular plunger of 380 mm^2 area to the surface of the saline bath. The flagellum, approximately 20 mm in length, was 7.5 mm beneath the saline surface; the plunger was centered over the flagellum, and its vertical movement to each pulse was about 25 μm and undoubtedly affected most if not all of the feathered sensilla. The black trace is an electronic average of 100 identical pulses delivered subsequently to the preparation. The electrical pulse to the speaker cone driving the plunger occurred at the start of the traces; spike volleys arrived at brain recording site beginning 5 ms following the stimulus onset, and a consistent pattern of volleys was present during a 5-ms time window thereafter. The stability and reproducibility of these and even later volleys is remarkable and attest to the rapid, reproducible responses of standing feathered sensilla to abrupt, near-field hydrodynamic stimuli in the vicinity of the antennular flagella.

Measurements of response latency and calculation of axonal conduction velocity

Examples of response latency measurements in sensillar axons are shown in Fig. 3A–F. Extracellularly recorded spikes were identified oscillographically by amplitude and waveform and from their consistent responses to mechanical stimulation of a visually identified feathered sensillum. As indicated in Fig. 3C,D, multiple spike responses greatly aided positive identification at the two recording loci.

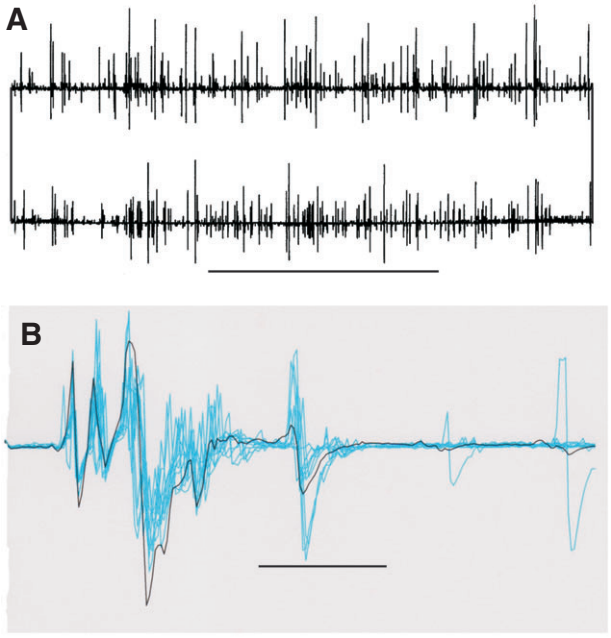

Fig. 2. (A) Spontaneous spiking activity recorded extracellularly from the medial branch of the antennular nerve at the flagellum base (upper trace) and at the entrance to the brain (lower trace). Most, if not all, of the activity arises from standing feathered sensilla. Time calibration bar, 500 ms. (B) Extracellular recordings from the medial antennular nerve at its entrance to the brain (in a different preparation from A). The cyan traces are superimposed responses to 10 consecutive individual 100-ms pulses delivered to the saline surface by a 380 mm^2 circular plunger positioned directly over a medial flagellum at an approximate vertical distance of 0.75 cm. The black trace is an electronically averaged response to100 identical 100-ms stimulus pulses delivered at 0.5 Hz. Time calibration bar, 10 ms. See text for further discussion.

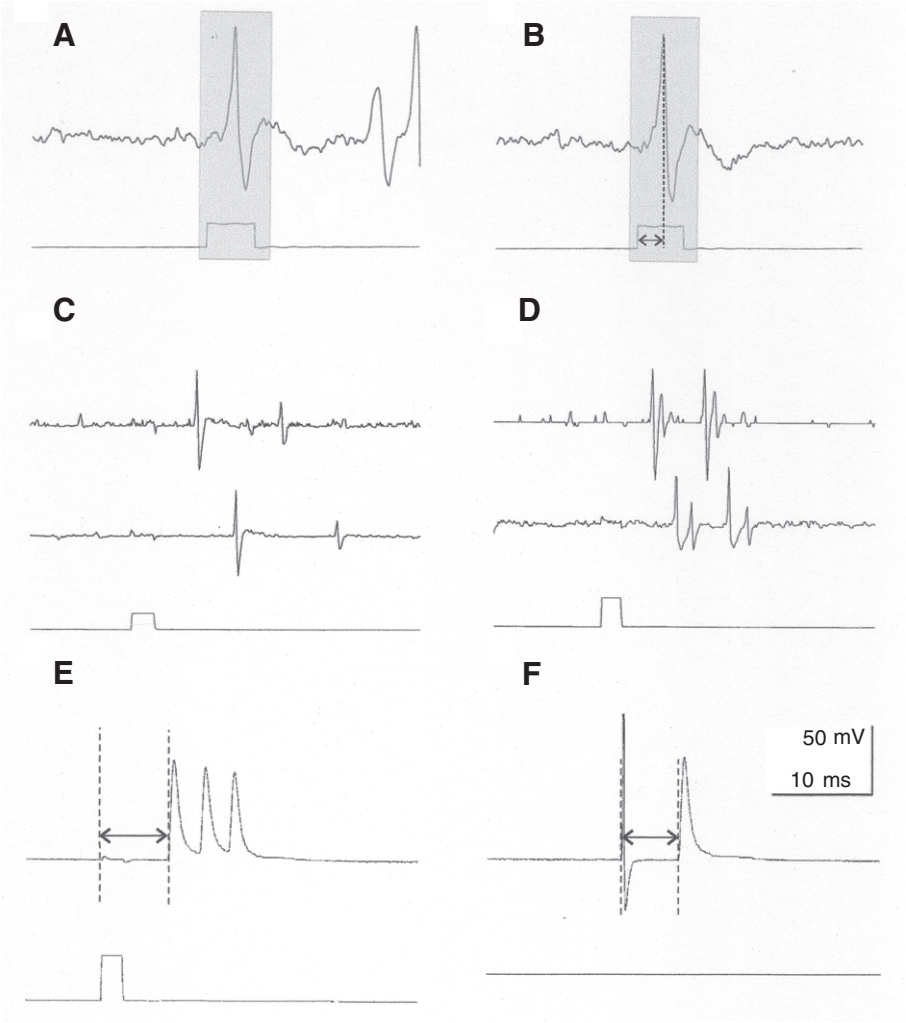

Fig. 3. Explanation of the technique used to determine spike latencies from isolated flagella and from antennular nerves in head preparations. (A,B) spikes from individual sensilla (top traces, shaded regions) were recorded by an extracellular electrode at the base of a flagellum and are visually identifiable on the basis of amplitude and waveform. Bottom traces show the mechanical stimulus pulses of 2 ms duration. The time period used to measure spike latency is shown in B. Occasional impulses from other, non-stimulated sensilla are also present. (C,D) Simultaneous extracellular records from the medial antennular nerve branch at the flagellum base (top traces) and the entrance to the brain (bottom traces) following a 2-ms mechanical stimulus to the sensillum associated with the prominent axonal spikes. Initial spike latencies were measured as in B. (E,F) Intracellular recordings from a feathered sensillum axon obtained from a penetration in the antennular nerve near the brain. Spikes are shown in response to, respectively, mechanical and electrical stimulation. Mechanical pulse (lower trace) duration in E was 2 ms. Latency measurements were made using the time windows indicated by the double-headed arrows.

Fig. 3E,F illustrate the latency parameters used to compare mechanically and electrically evoked activity in the same sensillar axon, the results of which are shown in Table 1 for 11 sensilla. These comparisons were necessary to determine whether a significant proportion of the mechanically evoked response latency was due to 'activation time', the time between the onset of the electrical pulse to the probe speaker and the initiation of the first conducted action potential in the sensillar axon, and assuming that the activation time following electrical stimulation of the same axon at the sensillum was negligible. As shown in Table 1 the differences in latencies of the two stimulation techniques varied among preparations, from a minimum value of 0.31 ms to a maximum of 2.21 ms. The mean of the difference between the two methods in the eleven axons was 1.54 ms.

Initial spike latencies in response to stimulation *via* the speaker probe were recorded simultaneously at the brain and from the medial branch of the antennular nerve at the base of the medial flagellum. I obtained measurements from 40 identified sensilla in 15 different preparations, in which the range of medial flagellar length was 21.5–29.9 mm. The results of latency measurements from the brain

Table 1. Comparison of mean response latencies following electrical and mechanical stimulation in 11 sensillar axons, using intracellular recording techniques

Axon	Flagellum	Sensillar annulus from base (mm)	Conduction distance (mm)	Temp (°C)	Electrical latency (ms)	Mechanical latency (ms)	Δ (ms)
12/17	Lateral	9	10	20	5.47	6.3	0.83
12/30 A	Lateral	45	24	19.5	12.4	13.73	1.33
12/30 B	Medial	29	20.5	19.8	5.35	6.35	1.00
01/06	Medial	9	8.8	18.3	4.67	6.66	1.99
01/07	Medial	14	12.4	19	4.3	6.51	2.21
01/09A	Medial	45	22.8	18.5	6.32	8.31	1.99
01/09B	Lateral	37	20	18.7	6.69	8.86	2.17
01/13A	Lateral	43	24.8	16.8	7.02	8.71	1.69
01/13B	Lateral	22	15.19	18.6	5.73	6.04	0.31
01/16A	Medial	10	12.25	15.3	7.21	9.16	1.95
01/16B	Lateral	53	26.35	18.3	7.63	9.16	1.52

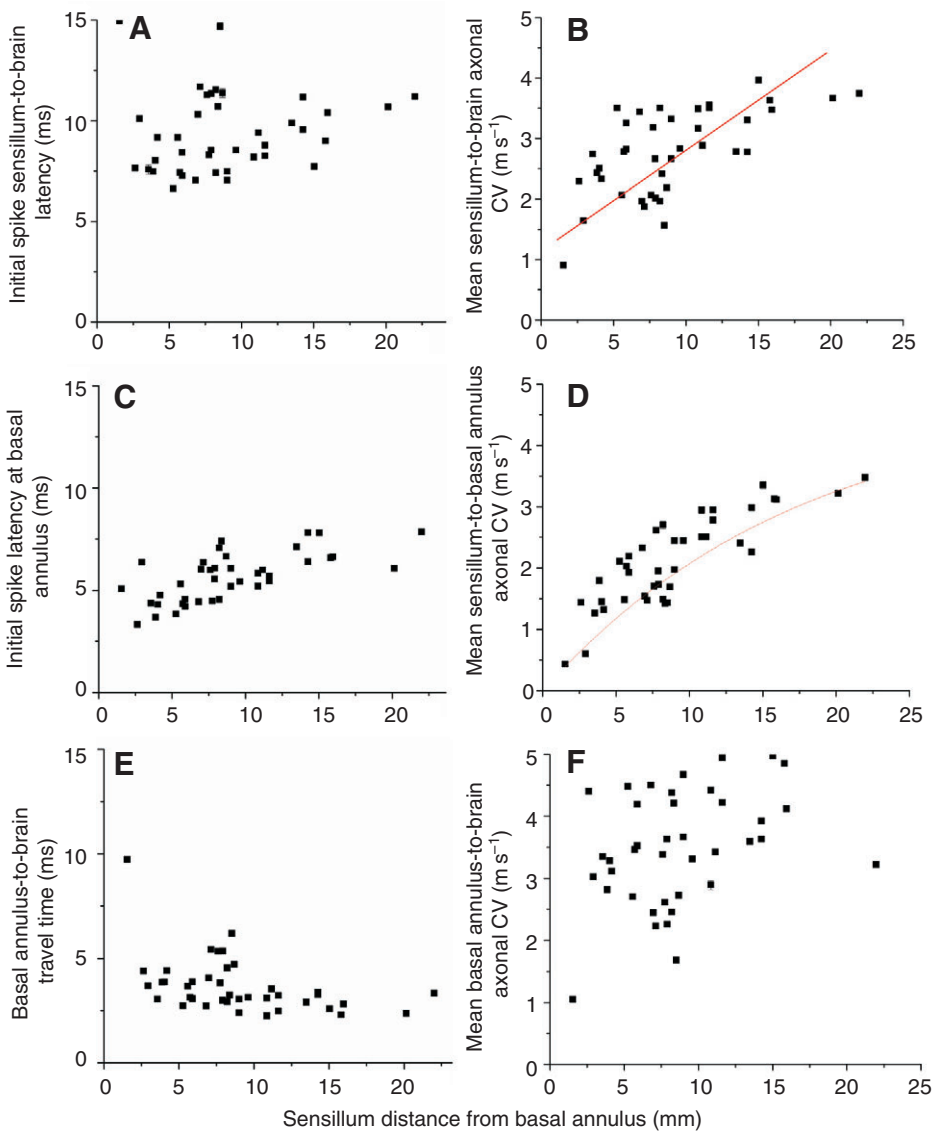

Fig. 4. (A,C,E) Initial spike latency and (B,D,F) mean CV data. Measurements were made directly from axons (A,B) between sensilla and the brain, (C,D) between sensilla and the flagellum base, and (E,F) between the flagellum base and the brain. The best fit of the sensillum-to-brain CV data is a linear function given by Y=0.16X+1.1, R=0.78, whereas that for the sensillum-to-basal annulus CV data is a first-order exponential: Y=–4.4 $e^{(-X/13.8)}$+4.4, R=0.93. Latency data obtained from four additional sensilla were not used because the standard deviation exceeded 15% of the mean value. See text for further description.

and basal annulus recording sites are shown, respectively, in Fig. 4A and C. All data points include an unknown activation time, as discussed above. There is little, if any, statistically significant relationship between initial spike latency at either the basal annulus of the flagellum or at the brain and the position of the sensillum of origin along the flagellum. Fig. 4E gives directly measured spike travel times between the basal annulus recording site and the brain recording site, simply by measuring the time interval taken by the identified spikes to be conducted between the two electrodes. These latency measurements did not include an activation time, which is undoubtedly part of the reason they are considerably shorter and have far less variance (mean coefficient of variation=1.5%) than those measured, for example, between the sensilla and the base (mean coefficient of variation=5.2%).

Mean CVs over the flagellar and basal segment pathways following mechanical stimulation were calculated using latencies that had been corrected for activation time by subtracting 1.5 ms from each measured value, prior to dividing the sensillum distances by them. The fact that the relationship between these latencies and sensillar position is essentially flat leads to a prediction that axons originating farther distally will exhibit faster mean CVs than those closer to the flagellum base. As found previously (Mellon and Christison-Lagay, 2008), this prediction was born out not only from calculations based upon latencies measured at the basal annulus (Fig. 4D) but also those measured at the entrance to the brain (Fig. 4B). Somewhat different from our previous findings, however, is that a first-order exponential relationship is a better fit to the data in Fig. 4D than a linear relationship, as found in Fig. 4B. Also surprising was the fact that the relationships between sensillar position and the calculated mean CVs of their corresponding axons disappeared when spike travel times were accurately measured between the flagellum base and the brain itself (Fig. 4F). In order to better determine the consequence of these data, I plotted flagellar mean axonal CVs against the corresponding mean base-to-brain CV of each axon. The results are shown in Fig. 5. There is a loose (slope=0.83X, R=0.62) linear relationship between the mean CVs within the medial flagellum and their corresponding values in the antennular nerve and suggests that axons with mid-range mean CVs (1–3 m s^{-1}) in the flagellum tend to increase their basal segment mean CVs (and, perhaps, their diameters) at a rate that is faster than those axons having relatively high flagellar mean CV; indeed, the slope of the linear relationship for CVs only within this middle range is 0.72. The relationship could account for some of the restricted temporal dispersion of initial spike arrival times at the brain that

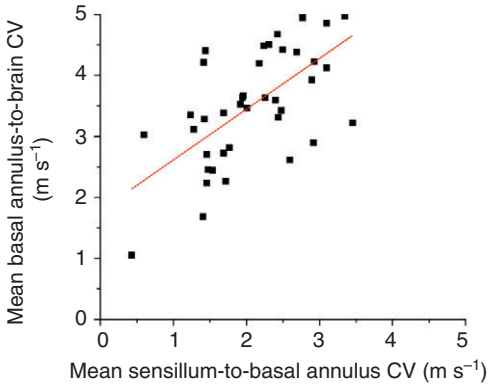

Fig. 5. Plot of basal-annulus-to-brain axonal CVs against the CVs from the sensilla-to-brain pathway. A best fit for the data is a linear function (Y=0.83X+1.8, R=0.62). A majority of the data indicate a higher axonal CV within the three basal segments of the antennule compared with CVs of the same axons within the flagellum.

would otherwise be predicted by the mean CV values calculated at the basal annulus.

Axonal diameters in the antennules

The dependence of axonal mean CV on sensillar position along the antennular flagellum described previously (Mellon and Christison-Lagay, 2008) and confirmed here could be exclusively due to increasing axonal diameters proximal to their point of origin. Transverse sections of medial flagella indicate that there is in fact a marked increase in diameter of some axons within the antennular nerve from a distal to proximal location along the flagellum (Fig. 6). One pair of axons could be followed in sections with a reasonable degree of confidence distally from the base to the point where they were no more than 2–3 μm in diameter. As described previously (Mellon and Christison-Lagay, 2008), the mean radius of this axon pair increased approximately 10-fold between the flagellum base and near the tip. In the current study, when similar histological techniques were used to examine and measure the mean diameters of the 20 largest axonal profiles in both the lateral and the medial flagellar branch of the antennular nerve within the three basal segments of two different antennules, however, the results were very different. Examples of transverse sections of the lateral branch of the antennular nerve from one preparation are shown in Fig. 7A,B, respectively, near the flagellum base and near the brain. Data obtained from the same preparation (Fig. 7C), show no net changes in mean diameter of the largest axon profiles between the base of the flagella and the brain.

DISCUSSION

Data presented here confirm and extend the axonal conduction velocity studies in antennular near-field receptors that we published previously (Mellon and Christison-Lagay, 2008). Axonal CVs between a sensillum and the base of an antennular flagellum increase

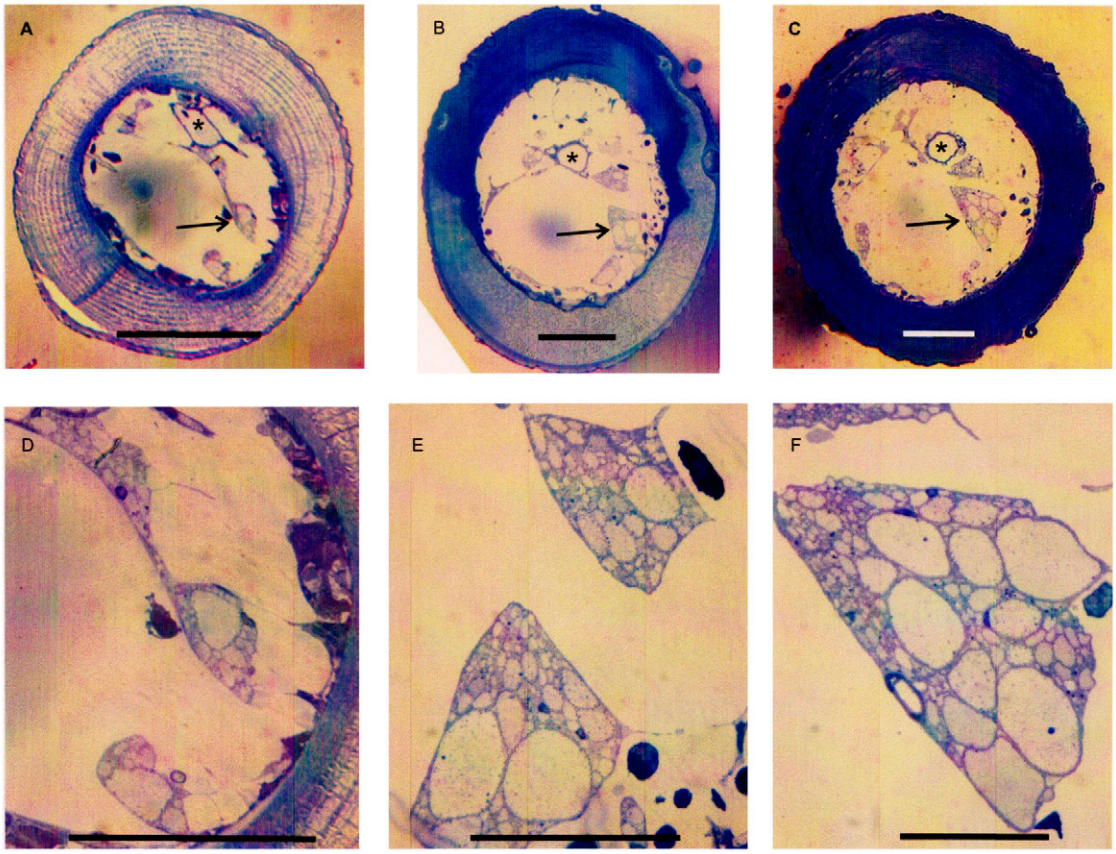

Fig. 6. Transverse sections through a medial antennular flagellum, cut at (A) 12.3 mm, (B) 3.0 mm and (C) 0.5 mm distal to the flagellum base. Note that the diameters of some axon profiles in the indicated nerve fascicles increase closer to the base. Asterisks indicate the medial branch of the antennular artery. (D–F) Enlargements of the imaged fascicles indicated by arrows in the corresponding section above each frame. Scale bars, 100 μm in A–C, 50 μm in D–F. F is reproduced with permission from Mellon and Christison-Lagay (Mellon and Christison-Lagay, 2008).

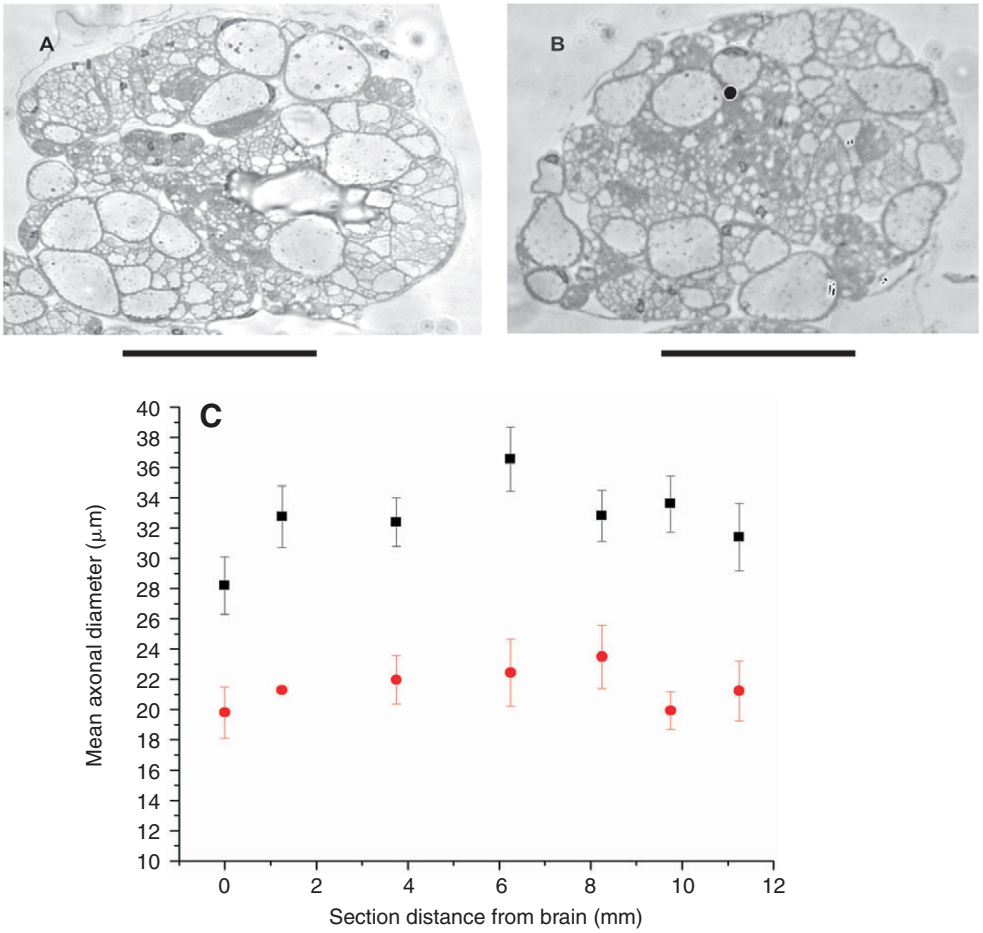

Fig. 7. Transverse sections through the lateral branch of the antennular nerve within the three basal segments, cut at (A) 11.25 and (B) 3.75 mm from the brain. (C) Plot of the mean diameter (±1 s.e.m.) of the 20 largest axons in sections from the medial (black squares) and lateral (red circles) branches of the antennular nerve taken at several points between the brain and the flagellum base. These probably account for most if not all of the feathered sensilla axons within the antennule. There does not appear to be any net change in axon diameter at the brain compared with that at the base of the flagellum. Scale bars, 50 μm.

with distance of the sensillum from the base, presumably, at least partly, because of an increase in axonal diameter along the flagellum, the cumulative effects of which will be greatest for the most distant sensilla. Because sensilla along the crayfish antennule increase in number as the animal grows, with new ones being added at the flagellum base and the oldest ones occurring distally (Sandeman and Sandeman, 1996), the oldest axons may have undergone a greater increase in diameter, as well as greater axial growth. From first principles, the membrane current density per unit area, I_m, associated with a propagating action potential in non-myelinated axons is given by the following equation:

$$I_m = a / 2R_i\theta^2 \, (d^2V / dt^2) \,, \quad (1)$$

where a is the axonal radius, R_i is axoplasm resistivity, θ is axonal CV, V is the membrane potential change associated with an approaching action potential, and t is time (Hodgkin and Rushton, 1946; Hodgkin, 1954). Since a/θ^2=constant (k), $\theta = ka^{1/2}$ and $\theta \propto \sqrt{a}$. Although these relationships describe differences in CV for axons having fixed diameters, it is possible to derive similar relationships for axons with expanding diameters. A recording electrode at the base of the antennular flagellum measures the response latency of an initial spike following a stimulus to its sensillum; corrected for activation time, this provides a measure of the *mean* conduction velocity, $\bar{\theta}$, along the axonal pathway between the sensillum and the electrode. Assuming a linear increase in diameter with distance from the sensillum, the mean axonal radius, $\bar{a}$, will be given by the following expression:

$$\bar{a} = (a_o + a_f) / 2 \,, \quad (2)$$

where a_o is the initial axonal radius at the sensillum and a_f is the final radius at the flagellum base.

If the relationship of mean CV, $\bar{\theta} = k\sqrt{a}$ holds, it can be shown through integration that:

$$\bar{\theta} = (k / 2) \, (a_f - a_o) \, [(a_f)^{1/2} - (a_o)^{1/2}]^{-1} \,. \quad (3)$$

In our previous study, we measured the increase in mean axonal radius for a pair of tentatively identified sensillar axons over a 15 mm length of medial flagellum, finding an approximate linear increase over that pathway, which was best fit by the equation Y=–0.61X+11.64, R=0.96, where Y is mean radius of the axon pair in micrometers and X is the distance of the section from the flagellum base in millimeters (Mellon and Christison-Lagay, 2008). The negative slope in the relationship is due to the fact that between the flagellum base and the distal site of axonal origin the radius decreases. I used the above equation to convert sensillum position to axonal radius, and calculated the relationships between measured mean CV and axon radius for each of the forty sensilla examined. The results are shown in Fig. 8. The relationship is best fit by the linear equation Y=0.2X+0.96, R=0.81. As shown by the open circles in Fig. 8, which was plotted from Eqn 3 using a_o=1 μm and a_f=15 μm, the measured mean CV increases faster with radius and differs from theoretical considerations based upon geometry alone; thus, the calculations suggest that other factors in addition to axonal diameter increase are responsible for the progressive increased CV as axons course within the antennular flagella. Other factors might include changes in the density of voltage-gated ion channels along the axon, which theoretically could accelerate development of action potential generation and, thus, its propagation along a nerve fiber. Such

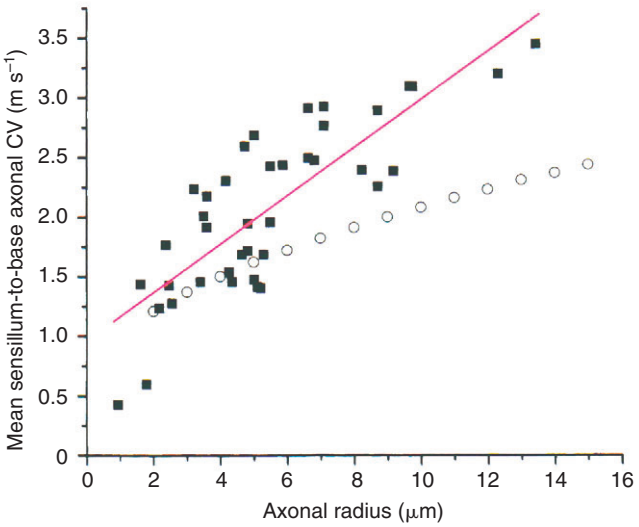

Fig. 8. Plots of mean measured (black squares) sensillum-to-basal annulus CVs against changes in axonal radius, using the linear fit of anatomical data (Y=–0.61X+11.64) obtained by Mellon and Christison-Lagay (Mellon and Christison-Lagay, 2008), and computed mean CVs (open circles) over the same range of radius changes using Eqn 3. The principal assumptions are that all axons have radii of 1 μm at their origin from the sensory neuron soma and increase their diameters linearly with distance from their position of origin. See text for further description of methods used.

changes in density are known to occur in single neurons from, for example, the mammalian central nervous system, where the density of voltage-gated sodium channels at the low-threshold axon hillock region of cortical neurons can be 50 times higher than along the proximal dendrites (Kole et al., 2008). Changes in voltage-gated ion channel kinetics can differ methodically among neighboring cells, as has been documented in vertebrate hair cells (e.g. Ramanathan et al., 1999), and this could potentially be a possible factor in regulating conduction velocity among axons of differing age. In vertebrate myelinated axons, CV is a linear function of axon diameter, and although some crustaceans such as shrimps and copepods, do have well-developed myelin wrappings along central or peripheral axons (Holmes et al., 1941; Kusano, 1966; Ritzmann, 1974; Lenz et al., 2000), myelin is not known to be present in the nervous systems of freshwater crayfishes, and there is no histological evidence for it in the antennular nerve of *P. clarkii*. For the present, therefore, the question of graduated CV regulatory mechanisms in the afferent fibers associated with crayfish feathered sensilla remains unanswered.

Feathered sensilla constitute a sparse population of setae along the antennule flagella; in a large crayfish only eight to 12 of this class of sensillum occur along the shaft of each flagellum. Although they are distributed along the entire length of a flagellum, the highest probability of occurrence is within the proximal 50% of its length (Mellon and Christison-Lagay, 2008). These sensilla are highly sensitive; displacements of as little as 0.02 μm constitute suprathreshold stimuli. The brain is therefore subject to a continuous barrage of spikes from these sense organs, much of which is probably noise and filtered out centrally. Spikes will be synchronized, however, by even low-level abrupt hydrodynamic inputs, which will activate a high percentage (if not all) of the available sensor population within a brief period of time: a prerequisite for triggering startle behavior (e.g. Wine and Krasne, 1972; Edwards et al., 1998). Initial spikes from most of the feathered sensillum population, therefore, should arrive at the brain within a brief time-window. Indeed, the superimposed records in Fig. 2B indicate that this is so following a global hydrodynamic stimulus to the antennule, with consistent spike signatures arriving at the brain within a 5-ms time window, *prima facie* evidence for temporal compression in initial spike arrivals over the afferent pathway. In the current study, the fastest CVs recorded at the flagellum base were about 3.5 m s^{-1}, and the slowest were 0.3 m s^{-1}. Using these values, 'back-of-the-envelope' calculations suggest that, over the 12–14 mm conduction distance between the flagellum base and the brain, the time taken for the fastest spikes to reach the brain would probably not exceed 3.5–4.0 ms, whereas that for the slowest axons would be 40–47 ms. Therefore, unless other CV adjustments were made, synchronous arrival of initial spikes from sensilla distributed along the antennular flagellum could not be achieved. What the present data show, however, is that this major dispersion does not occur; a majority of initial spikes at the brain are dispersed within a 5 ms time window, which is only slightly greater than the dispersion at the base of the flagella. A possible factor that has not been addressed (or measured) is the rate of diameter increase achieved by sensillar axons originating close to the flagellum base, as opposed to those associated with sensilla near the tip. If the basal axons increase their diameter abruptly in the most distal of the three base segments, their measured mean CV at the basal annulus could be deceptive, partially explaining the compression in spike arrival times.

Perhaps of equal importance to temporal compression of spike arrivals is the fact that hydrodynamic stimuli delivered to the entire flagellum generates highly consistent temporal patterns of initial spike volleys. Spiking activity in feathered sensilla neurons is inherently noisy. Against this background of dense, apparently random firing would appear to be the difficult task of distinguishing critically important signals having survival value. Brief, unique, recognizable patterns of input volleys from crucially important sensor populations may be plausible mechanisms to accomplish this formidable task. Recently, in an interesting study on the cercal filiform afferents in crickets, Mulder-Rossi et al. (Mulder-Rossi et al., 2010) found that, in striking contrast to the crayfish situation, axonal CVs from linearly-arrayed cercal sensilla are all similar and hence can act as delay lines. Sensory interneurons within the terminal abdominal ganglion of the cricket are activated by these afferents and, in some instances, are tuned to the sequential arrival of spikes in response to air currents moving at different directions and/or velocities with respect to sensillar array. In at least one case these sequential velocities are within the range known to elicit a backward kick from the cricket's metathoracic legs, a defense against approaching predaceous flies. However, these interneurons may ignore bulk air flow stimuli that simultaneously stimulates all filiform afferents, as would occur when the cricket moves voluntarily. I have not yet tested the effects of feathered sensilla on sensory interneurons within the crayfish brain, so the relevance of the cricket studies is unknown. An interesting question to pursue in future studies, however, is whether central targets of crayfish near-field afferents are tuned to the specific volley patterns following strong, abrupt hydrodynamic stimuli such as those produced by an approaching predator. Large bass can travel at velocities of 5–6 m s^{-1} (Davis and Lock, 1997), thereby nearly out-pacing the fastest sensillar axons. The extent to which the 'bow wave' of the approach precedes the predator itself will have a direct bearing on the margin of escape available to the crayfish. Addressing these considerations

will further the understanding of the properties of antennular hydrodynamic sensilla in relation to behavior.

ACKNOWLEDGEMENTS

I am indebted to my colleague, Dr W. Otto Friesen, for deriving the relationship in Eqn 3 and for his helpful insights and discussion on theoretical considerations in action potential propagation. I am grateful to Ms Alana Colton for collecting and analyzing preliminary axonal conduction velocity data, to Ms Jan Redick for technical assistance with histological preparation of the antennular nerve sections, and to two anonymous reviewers whose careful and penetrating attention to the original manuscript have significantly improved its focus and content. Finally, thanks are due the staff of the MBL-WHOI library at the Marine Biological Laboratory in Woods Hole, Massachusetts for their help with reproducing some of the text figures. This research was supported in part by research grant CBET-0933034 from the National Science Foundation.

REFERENCES

Davis, J. T. and Lock, J. T. (1997). *Largemouth Bass: Biology and Life History*. Publication No. 200 from the Southern Regional Aquaculture Center.

Edwards, D. H., Yeh, S. R. and Krasne, F. B. (1998). Neuronal coincidence detection by voltage-sensitive electrical synapses. *Proc. Natl. Acad. Sci. USA* **95**, 7145-7150.

Hodgkin, A. L. (1954). A note on conduction velocity. *J. Physiol.* **125**, 221-224.

Hodgkin, A. L. and Rushton, W. A. H. (1946). The electrical constants of a crustacean nerve fibre. *Proc. R. Soc. Lond. B. Biol. Sci.* **133**, 444-479.

Holmes, W., Pumphrey, R. J. and Young, J. Z. (1941). The structure and conduction velocity of the medullated nerve fibers of prawns. *J. Exp. Biol.* **18**, 50-54.

Kole, M. H. P., Ilschner, S. U., Kampa, B. M., Williams, S. R., Ruben, P. C. and Stuart, G. J. (2008). Action potential generation requires a high sodium channel density in the axon initial segment. *Nat. Neurosci.* **11**, 178-186.

Kusano, K. (1966). Electrical activity and structural correlates of giant nerve fibers in kuruma shrimp (*Penaeus japonicus*). *J. Cell. Physiol.* **68**, 361-384.

Lenz, P. H., Hartline, D. K. and Davis, A. D. (2000). The need for speed. I. Fast reactions and myelinated axons in copepods. *J. Comp. Physiol. A Physiol.* **186**, 337-345.

Mellon, DeF. (1997). Physiological characterization of antennular flicking reflexes in the crayfish. *J. Comp. Physiol. A* **180**, 553-565.

Mellon, DeF. and Christison-Lagay, K. (2008). A mechanism for neuronal coincidence revealed in the crayfish antennule. *Proc. Natl. Acad. Sci. USA* **105**, 14626-14631.

Mulder-Rosi, J., Cummins, G. I. and Miller, J. P. (2010). The cricket cercal system implements delay-line processing. *J. Neurophysiol.* **103**, 1823-1832.

Ramanathan, K., Michael, T. H., Jiang, G. H., Hiel, H. and Fuchs, P. A. (1999). A molecular mechanism for electrical tuning of cochlear hair cells. *Science* **283**, 215-217.

Ritzmann, R. E. (1974). Mechanisms for the snapping behavior of two alpheid shrimp, *Alpheus californiensis* and *Alpheus heterochelis*. *J. Comp. Physiol.* **95**, 217-236.

Sandeman, D. C. and Luff, S. E. (1974). Regeneration of the antennules in the Australian freshwater crayfish *Cherax destructor*. *J. Neurobiol.* **5**, 475-488.

Sandeman, D. C. and Sandeman, R. E. (1996). Pre- and postembryonic development, growth and turnover of olfactory receptor neurons in crayfish antennules. *J. Exp. Biol.* **199**, 2409-2418.

Tierney, A. J., Thompson, C. S. and Dunham, D.W. (1986). Fine structure of aesthetasc chemoreceptors in the crayfish *Orconectes propinquus*. *Can. J. Zool.* **64**, 392-399.

Wine, J. J. and Krasne, F. B. (1972). The organization of escape behaviour in the crayfish. *J. Exp. Biol.* **56**, 1-18.